




Article

Double-Skin Façades for Building Retrofitting and Climate Change: A Case Study in Central Italy

Camilla Lops , Samantha Di Loreto, Mariano Pierantozzi  and Sergio Montelpare 

Department of Engineering and Geology, University G. d'Annunzio of Chieti-Pescara, 65122 Pescara, Italy; samantha.diloreto@unich.it (S.D.L.); mariano.pierantozzi@unich.it (M.P.); s.montelpare@unich.it (S.M.)

* Correspondence: camilla.lops@unich.it; Tel.: +39-085-453-7258

Featured Application: Forecast procedures for building energy renovation and design.

Abstract: In recent years, the need to make the built environment more resilient and adaptable to climate change has become essential. In Europe, this aspect concerns most existing buildings with several deficiencies from the energy efficiency point of view, considering they were designed before the introduction of modern codes. Among the various strategies for building energy retrofitting, Double-Skin Façades (DSFs) have gained attention due to their potential to improve the building performance and inhabitants' comfort. This research aims to evaluate the use of adequately designed DSFs for the energy restoration of buildings. In detail, various DSF configurations are applied to a residential building located in Central Italy and investigated under present and future climate conditions, estimated through regional climate models. The installation of multi-layered façades, particularly the Multi-Storey typology, greatly reduces energy consumption and increases the expected comfort rates. When the selected configuration was considered, the results underline a decrease in the annual building energy requirement of about 37–56% up to 42–59%, respectively, for 2030 and 2070. Moreover, using multi-layer façades can increase indoor minimum operative temperatures up to 3.8% during the coldest months and reduce the maximum summer ones by 1.9–3.8%, raising comfort levels.

Keywords: building energy retrofitting; Double-Skin Façades; climate change; regional climate model; dynamic energy modelling; MM5; CORDEX



Citation: Lops, C.; Di Loreto, S.; Pierantozzi, M.; Montelpare, S. Double-Skin Façades for Building Retrofitting and Climate Change: A Case Study in Central Italy. *Appl. Sci.* **2023**, *13*, 7629. <https://doi.org/10.3390/app13137629>

Academic Editor: Paulo Santos

Received: 3 June 2023

Revised: 24 June 2023

Accepted: 26 June 2023

Published: 28 June 2023



Copyright: © 2023 by the authors. Licensee MDPI, Basel, Switzerland. This article is an open access article distributed under the terms and conditions of the Creative Commons Attribution (CC BY) license (<https://creativecommons.org/licenses/by/4.0/>).

1. Introduction

In recent decades, the economy centred on the general reduction in energy consumption and CO₂ emissions has dictated important changes in every sector, especially in the construction world. Buildings are, in fact, key consumers of energy in Europe, and a rising tendency in energy use has been globally recorded in the last twenty years [1]. According to the European Environment Agency (EEA), in 2017 the transport sector accounted for 31% of the total final energy consumption in the European Member States, followed by households (27%), industry (25%) and services (15%) sectors [2].

The energy use in households is mainly related to space and water heating, which together are responsible for 80% of the total building energy consumption [3]. This high percentage is mostly due to poorly insulated envelopes and less-efficient heating equipment, which are mainly fossil-fuel-based and traditionally present in existing buildings.

Similar trends are also estimated for greenhouse gas emissions. Buildings and construction together account for 39% of energy-related CO₂ emissions when upstream power generation is included [4]. Considering the high potential for cost-effective energy savings, the building sector has become a priority area for the European Commission, which has sponsored various actions to reduce the building requirement and promote their renovation. Prominent examples of this effort are the Directive 2002/91/EC [5] and the Directive

2010/31/EU [6], commonly known as the EPBD (from its full name the Energy Performance of Buildings Directive) and its recasting. The first is mainly centred on defining a standardised methodology more oriented to new buildings. The second, on the other hand, aims to deal with existing buildings not only when they are subjected to a significant renovation but also in replacing and retrofitting a few elements or technical systems. After the EPBDs, the European Member States have shown a growing interest in building energy improvement, and, as a main result, a specific article centred on building renovation was introduced in the new Energy Efficiency Directive 2012/27/EU [7].

The great interest in the existing building stock is due to the fact that most European buildings currently in use were erected before the 1960s when the sustainability problem was in a preliminary phase, and energy building regulations were minimal. According to the Building Performance Institute Europe (BPIE) survey, in fact, 35–42% of these buildings date back to before the 1960s, and another consistent part was erected between 1961 and 1990 due to the massive boom in the construction sector [8]. The statistics underline the need for energy-efficient retrofit solutions, which are essential under present and, in particular, future conditions, considering that the construction age of a building is among the main features that affect its climate change vulnerability. Various innovations for improving the energy performance of buildings and, generally, cities, to reduce their environmental impact involve smart and intelligent devices, which are mostly renewable-based and installed directly on building surfaces [9,10] or at an urban scale [11–13].

In this way, the present research aims to evaluate the climate change vulnerability of an existing building in Central Italy by estimating its energy needs and comfort rates under future meteorological conditions and considering both the current and energy-improved versions. In detail, the investigated retrofit solutions take into account the installation of Double-Skin Façades (DSFs) on the building's main elevations, and we analyse multiple configurations to assess the best typology for the specific climatic area. The novelty of the work lies, in particular, in locating the multi-layer façade on more than one elevation. Generally, in fact, DSF systems are placed on only one façade, the north one, and designed to act as a filter zone [14–18]. Instead, a so-conceived configuration could also assume a structural purpose after the installation of seismic devices, in pursuit of the building's holistic renovation. A second innovative aspect of the work is related to the selection of the climatic parameters adopted for the analyses, which are usually performed using historical or current datasets [19,20]. Studying DSF systems under future weather conditions allows the estimation of their sensitivity to climate change phenomena, underlining their potentiality and weakness. The above-mentioned features are analysed using performing dynamic energy simulations in EnergyPlus (Version 8.9) with its DesignBuilder interface (Version 6.1.3).

In detail, the paper is structured as follows. After this brief introduction, considerations of Double-Skin Façades and their use in new and retrofitted buildings are reported in Section 2. Section 3 describes the case study, the main energy modelling features and the preliminary simulations carried out for testing the model's capability in predicting the real energy behaviour of the reference building. Section 4 focuses on the presentation of the methodology adopted for generating future climatic files and shows the obtained results expressed in energy consumption and comfort rates. A discussion of the outputs is described in Section 5. Finally, Section 6 draws the main conclusions.

2. Double-Skin Façades for New and Retrofitted Buildings

The Double-Skin Façade is an architectural trend mainly driven by the aesthetic desire for all-glass façade buildings, the need for a consistent reduction in energy consumption and the parallel increase in indoor comfort conditions, both acoustic and thermic [21]. Described as a pair of glass skins separated by an air corridor ranging in width from 0.20 m to several meters by Uuttu [22], the DSF concept appeared in the early 20th century in northern European countries as a way to reduce heating consumption thanks to the air buffer enclosed in the cavity, which acts as a barrier for heat loss and as a filter for exchanges through the external envelope. The extreme variety of possible DSF typologies

can be classified according to different criteria, independent of one another and based on the geometric characteristics of the façade and its operation mode [23]. The criteria mentioned above are the following:

- The ventilation mode (natural, mechanical and hybrid ventilation).
- The compartmentalisation of the façade (Multi-Storey, Shaft-Box, Corridor and Box-Window DSF).
- The airflow type (Exhaust Air, Supply Air, Static Air Buffer, External Air Curtain, Internal Air Curtain).

In the second decade of the 21st century, more articulate configurations and advanced materials started to be combined with multi-layer systems to enhance their energy performance, and more accurate simulation approaches were adopted to overcome modelling limitations and difficulties [24–26].

Nowadays, the analysis of solutions for improving the energy behaviour of Double-Skin Façades is a topic frequently explored by researchers all over the world. Detailed investigations are conducted to evaluate DSFs' efficiency when different glazing options and shading systems are used. According to the literature review [27], using single clear glass for the inner pane and double reflective glazing for the outer surface is the best option, with annual cooling savings of up to 26% compared to a traditional external wall and single absorptive window glazing. Another essential and widely analysed aspect involves the shading system and the main parameters responsible for better solar protection. According to Gratia et al. [28], in fact, building cooling energy consumption can be decreased by up to 23% by paying attention to three main aspects: the location of the blinds, the colour of the blinds and the opening of the Double-Skin. Other investigations involve possible connections of DSFs with the Heating, Ventilation and Air Conditioning (HVAC) system, its use as a solar chimney or the installation of new elements like Photovoltaic (PV) cells, vegetation, or Phase-Changing Materials (PCMs) [29–39].

DSF innovation does not involve only energy efficiency aspects. A novel area of focus is the installation of structural elements able to confer an extra function, a seismic one, to the so-called Engineered Double-Skin Façade [40–45]. Such a façade becomes a mass damper system or an exoskeleton, which, in the case of restoration, can reduce the seismic vulnerability of existing buildings.

Based on the considerations mentioned above, multi-layer façades represent interesting options for both new and retrofitted buildings. In fact, several works study the improvements achievable by installing DSF systems in existing buildings, underlining their key role in cutting building energy consumption and CO₂ emissions if properly designed and oriented [46–49].

3. The Case Study

The reference building is located in a residential suburb of Pescara, Central Italy, and belongs to the social housing stock (Figure 1). Selected for being representative of an existing building without architectural quality but mostly present on the territory, it reflects the typical construction practice of the past, with no consideration of energy problems. The area is known for its Mediterranean climate, with mild winters and hot, sunny summers. According to the climate classification system developed by Köppen–Geiger [50], the city has a humid subtropical climate denominated Cfa. The C group corresponds to “Warm Temperate” climates; the small letter f means “fully humid” and indicates the lack of a dry season, whereas the letter a corresponds to a “hot summer”.



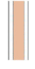




The case study is a seven-storey reinforced concrete building characterised by a rectangular shape with 60.00 m and 12.00 m as its main dimensions. The interstorey height is 2.70 m, except for the ground floor, which is higher than the others (3.50 m). The garages and the entrance are on the ground floor, while residential apartments are on the upper levels. The building envelope does not comply with the current standard in the sector. The perimeter walls (0.33 m depth), in fact, do not present any insulation materials but only an air gap enclosed by two brickwork layers, with a total transmittance value (U) equal to

1.46 W/m²K. There are also 0.23 m thick walls placed to delimit the apartment from the staircase, and partitions (with 11 cm of depth) to subdivide each apartment into various thermal zones. Moreover, single glass windows with 3.78 W/m²K transmittance contribute to the building's inadequate performance, especially during the coldest months. Table 1 summarises the thermal properties of the building envelope.



Figure 1. The localisation of Pescara (**left** and **middle**) and the reference building (**right**).

Table 1. Description of building envelope components.

Building Component	Material (Outer to Inner)	s (m)	l (W/mK)	U (W/m ² K)
0.33 m External Wall 	Lime plaster	0.02	0.80	1.46
	Brickwork	0.13	0.84	
	Air gap	0.08	0.30	
	Brickwork	0.08	0.62	
	Lime plaster	0.02	0.80	
0.23 m Semi-External Wall 	Lime plaster	0.02	0.80	1.60
	Brickwork	0.13	0.84	
	Air gap	0.03	0.30	
	Brickwork	0.08	0.62	
	Lime plaster	0.02	0.80	
0.11 m Partitions 	Plaster	0.02	0.16	1.27
	Plasterboard	0.07	0.25	
	Plaster	0.02	0.16	
Glazing 	Single clear glazing	0.006	-	3.78
Interstorey roof 	Cast concrete	0.02	1.13	0.78
	Concrete slab	0.16	0.16	
	Plaster	0.02	0.16	
External roof 	Ceiling tiles	0.02	0.06	0.61
	Cast concrete	0.02	1.13	
	Concrete slab	0.16	0.16	
	Plaster	0.02	0.16	
Pavement 	Cast concrete	0.02	1.40	3.37
	Ceramic	0.02	1.30	

The building heating system involves the use of radiators with a seasonal Coefficient of Performance (COP) equal to 0.84 and natural gas as the source. Splits are installed to

cool the inner spaces and improve the inhabitants' comfort condition. The cooling COP is set equal to 1.40, and the source is electricity.

The temperature setpoints for heating and cooling are, respectively, 22 °C (with 20 °C as the set-back temperature) and 28 °C in all thermal zones. The metabolic factor is set to 0.90 for the whole building, as well as for the clothing insulations, which is 0.50 clo for the summer season and 1.00 for the winter period. The model infiltration is considered to be constant and fixed at 0.70 ac/h. Table 2 depicts the input parameters, which vary according to the activity of the thermal zone.

Table 2. The main input parameters assigned to each thermal zone.

Thermal Zone	Occupation (People/m ²)	Fresh Air (l/s per Person)	Illuminance (Lux)	Schedule (-)
Bedroom	0.0229	10	100	
Bathroom	0.0187	12	150	
Kitchen	0.0237	12	300	
Storage Room	0.0243	12	100	
Dining Room	0.0169	10	150	
Circulation Area	0.0196	10	100	

The influence of neighbouring buildings is taken into account by inserting, as block components, the closest structures that could shade the case study and, for the same reason, the balconies on the northwest façade are considered by placing external profiles. Figure 2 shows the main elevations of the elaborated energy model.

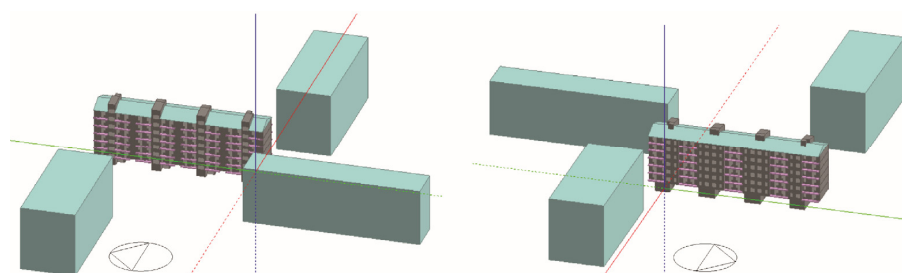


Figure 2. Northwest (left) and southeast (right) views of the energy model generated in DesignBuilder.

Once the case study had been modelled, preliminary dynamic energy simulations were carried out, and the building's natural gas consumption was estimated and compared with data from building bills. The collected bills refer to 2017, and the heating period (1 October–31 March) was considered for the comparisons. Thus, monthly simulations were performed, setting natural gas consumption (heating + cooking) as a key output, expressed in kWh/m². Following the recorded data, the consumption was determined for a two-month range, except for January and December. The analyses were simulated using measured weather data collected by the Climate Network, a private and professional network of urban meteorological stations that record hourly values for all climatic parameters [51]. Error bars, set at 5%, were inserted as inferior and superior limits.

Figure 3 shows the general accordance between estimated and measured values. The model, in fact, can predict within an acceptable range the energy consumption for January and the February/March bimester. More significant differences were calculated for December. Such behaviour can be explained by considering that the available bill refers to December 2017–January 2018, and the expected consumption for a single month is calculated by dividing the total amount by two. For this reason, the December data were not strictly taken into account for this step. The same inaccuracy can also be seen for the October/November bimester, but, in this case, the principal reason is the limitation of predictions for transitory months because these are deeply influenced by the inhabitants' comfort condition and their use of occupied spaces. In fact, as underlined by various works previously carried on in energy simulations, the building requirement/consumption for mild periods could vary more than the rest of the year, according to human behaviour (inhabitants' age, habits, etc.). It is essential to bear in mind that, considering the cumulative value (bimonthly) of measured data, which are related to a specific apartment located inside the building under analysis, a global comparison, rather than a monthly calibration, was performed. Nevertheless, by applying the ASHRAE guideline 14 criteria only to the accurate data, the Normalised Mean Bias Error (NMBE) and the Coefficient of Variation of the Root Mean Square Error (CVRMSE) were determined, respectively, to be 1% and 0% for January and −3% and 3% for the February/March bimester, which are both inside the acceptable range established by the standard. Based on these comparisons, the model can be considered able to describe the real energy behaviour of the case study.

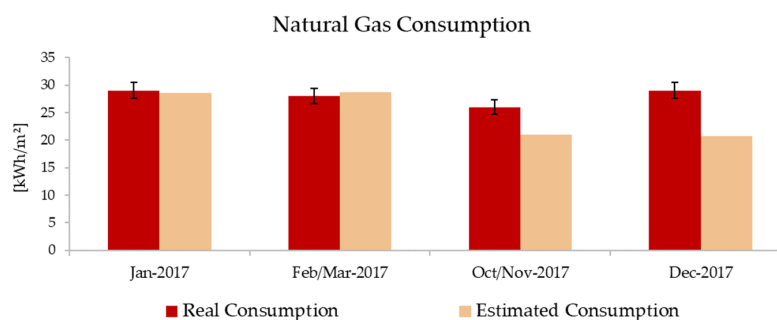


Figure 3. Comparisons among estimated and measured data.

DSF Energy Modelling

A Double-Skin Façade with a 1.00 m cavity depth is installed on the northwest and southeast building elevations, and external blinds with low reflectivity slots are installed and designed to be operable only during the hottest months, thus preventing the risk of overheating the inner spaces. The DSF is designed to be naturally ventilated. External and internal grills are located, respectively, on the outer skin and the inner layer, represented by the existing building envelope. External grills are active, allowing the air to enter the Double Façade during the hottest months, whereas they are closed for the winter period, creating a buffer area. The internal grills, instead, are designed to be adjustable according to the inner temperature distribution. The natural ventilation of the building is controlled by conducting an outdoor maximum temperature check. This prevents overheated air inside the cavity from entering the building and having adverse effects on the cooled side. The outer skin of the DSF is made of a steel structure and high-performance windows composed of triple glazing (a 13 mm cavity filled with Argon gas sealed by two layers of 3 mm single clear glass) with a low U value and solar heat gain coefficient equal to, respectively, $0.78 \text{ W/m}^2\text{K}$ and 0.47 . The DSF inner partitions, both horizontal and vertical, present steel frame and single-pane windows made of 6 mm clear glass with a transmittance and solar heat gain coefficient of $3.78 \text{ W/m}^2\text{K}$ and 0.72 .

The energy modelling of the DSF was achieved by setting the cavity as an unoccupied zone with no HVAC or lighting template data. Moreover, the internal convection mechanism was activated to model the cavity air space correctly, and a complete interior and exterior solar distribution algorithm was switched on, allowing solar radiation to be accurately transmitted through the interior glazing in the partition.

Various configurations were modelled and tested to evaluate the effectiveness of DSF systems. Multi-Storey, Shaft-Box, Corridor and Box-Window DSFs were investigated in terms of energy consumption and thermal comfort conditions. Two different cases were studied for the Corridor type: the outer grills were inserted on the principal elevation of the façade in one case and on the lateral envelope in the other. The inner partitions, which were eventually inserted inside the cavity according to the selected category, present single-glazed windows enclosed in a steel structure. Figure 4 schematises the chosen options, identifying the air fluxes which enter/exit each DSF typology.

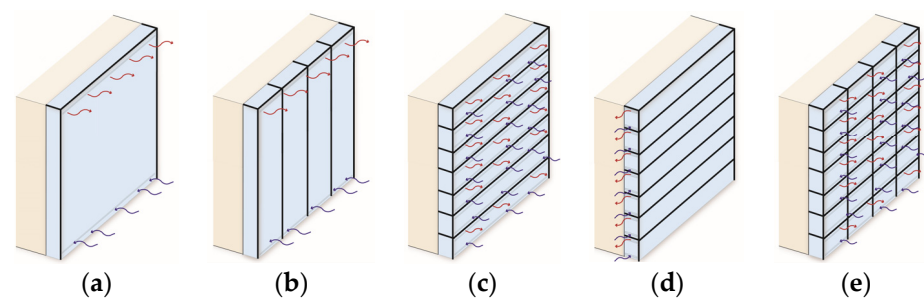
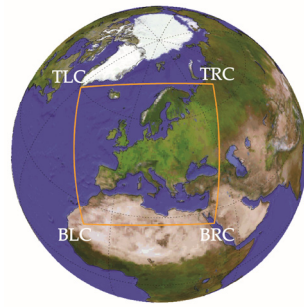


Figure 4. Schematisation of the investigated Multi-Storey (a), Shaft-Box (b), Corridor (c,d) and Box-Window (e) DSFs.

4. Dynamic Energy Simulations under Future Climate Conditions

4.1. Generation of Future Climatic Files for Dynamic Energy Simulations

Future climatic files are generated by using the Coordinated Regional Climate Downscaling Experiment (CORDEX). Sponsored by the World Climate Research Program (WCRP) to develop a coordinated framework for evaluating and improving Regional Climate Downscaling (RCD) techniques, CORDEX produces worldwide fine-scale climate data [52]. The CORDEX results are assumed as a baseline by the Intergovernmental Panel on Climate Change (IPCC) to define climate change impact and adaptation studies. Its various domains allow the estimation of meteorological variables all over the world, and the Euro-CORDEX, reported in Figure 5, is its European branch.



Non-Rotated Coordinates of Domain Corners

Top Left Corner (TLC): 315.86; 60.21

Top Right Corner (TRC): 64.4; 66.65

Bottom Left Corner (BLC): 350.01; 22.20

Bottom Right Corner (BRC): 36.30; 25.36

Figure 5. Euro-CORDEX Domain and the coordinates of its corners.

The Aire Limitée Adaptation dynamique Développement InterNational (ALADIN), used at the Centre National de Recherches Météorologiques (CNRM) with the name CNRM-ALADIN and available in Euro-CORDEX was selected in the present work [53,54]. This limited-area bi-spectral model was chosen due to its capability to predict with good approximation climatic parameters both spatial and temporal scales inside the European area [55,56]. Thus, data with a 3 h time frequency were extracted from the nearest grid point to Pescara, which is 7.50 km from the case study, at $42^{\circ}28'57''$ northern latitude and $14^{\circ}08'07''$ eastern longitude. The selected RCP was 4.5, which is consistent with a future with relatively ambitious emission reductions, and this scenario was chosen for being in accordance with national policies centred on reducing greenhouse gas emissions.

The available weather variables were relative humidity, atmospheric pressure, global solar radiation, wind velocity and temperature. The definition of the reference year was conducted according to the method described in the technical standard EN ISO 15927-4:2005 [57] and following its suggestions [52,58]. Multiple years were extracted to obtain various typical years.

The first step involved the calculation of the daily averaged value for each climatic parameter (p), month (mt) and year (y) of the datasets. Then, the averaged values for a specific month in all the available years were sorted in increasing order to calculate the cumulative function $\phi_{(p,mt,i)}$ for each parameter and i th day using Equation (1).

$$\phi_{(p,mt,i)} = k_{(i)}/N + 1 \quad (1)$$

where $k_{(i)}$ is the rank order of the i th day and N is the total number of days in a month across all years.

The following step consisted of sorting the averaged values for a specific month and year in increasing order to obtain the cumulative distribution function $F_{(p,y,mt,i)}$ for each parameter and i th day (Equation (2)).

$$F_{(p,y,mt,i)} = J^{(i)}/n + 1 \quad (2)$$

Then, for each month and year, the statistics by Finkelstein–Schafer were defined according to Equation (3). The last two steps involved the sorting of months, for which the rank was calculated for every parameter and summed to obtain the total ranking and for each month. Among the first three months with the lowest ranking sum, the one with the lower absolute deviation was chosen as a representative for the TMY generation.

$$Fs_{(p,y,mt)} = \sum_{i=1}^n \left| F_{(p,y,mt,i)} - \phi_{(p,mt,i)} \right| \quad (3)$$

To improve the quality of the generated TMY, weighted meteorological parameters were inserted in the Finkelstein–Schafer, as suggested by Cebeacauer et al. [58]. The stronger influence of some variables than others is taken into account by increasing the weight of those parameters. Higher impact factors are attributed to surface temperature and solar radiation (8/24), whereas a lower value (4/24) is assigned to relative humidity and wind speed, which slightly affect energy simulations. A twenty-year range was selected to generate a typical year. Thus, data from 2020 to 2040, 2040 to 2060 and 2060 to 2080 were

used to elaborate, respectively, 2030, 2050 and 2070 TMYs. Once the selected years were generated, a cubic spline function was used to obtain interpolated values and transform the time frequency of the investigated parameters from 3 h to 1 h.

Figures 6 and 7 depict comparisons of monthly mean values for temperature and global solar radiation between actual (Climate Network database) and future (2030, 2050 and 2070 TMYs) climate data. The future conditions (dotted lines) tended, in general, to assume similar values and trends to those measured in 2017. According to the predictions, higher temperatures are expected for the coldest months (from November to February), while a slight reduction is estimated for summer. More profound variations are expected, instead, for global solar radiation. In this case, the values estimated by CORDEX TMYs are much higher than those recorded in the present, reaching up to 330 W/m^2 .

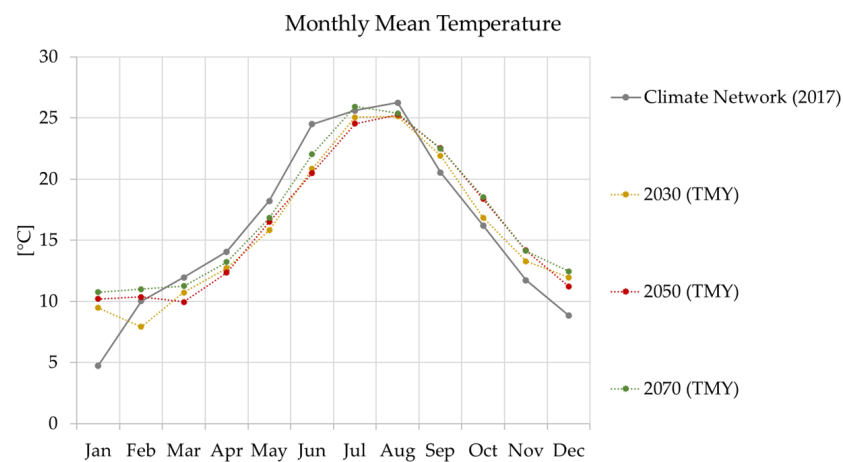


Figure 6. Monthly mean values referring to the temperature.

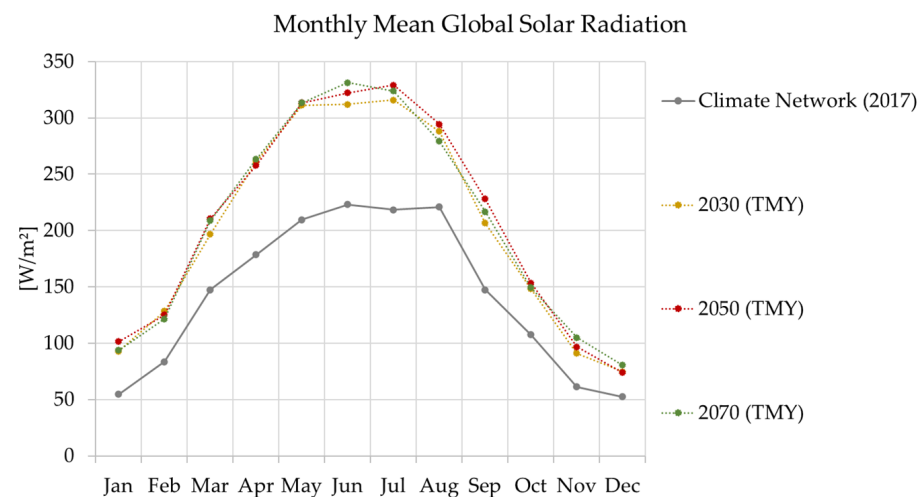


Figure 7. Monthly mean values referring to global solar radiation.

The same trend was confirmed by comparing these parameters to early averaged values (Figure 8). On the temperature side, from actual to future conditions, the increase is gradual, reaching a 2 °C delta between 2017 and 2070, whereas higher variation is expected for solar radiation. It is essential to underline that these comparisons involve projections related to a specific scenario which considers the adaptation of policies for CO_2 emission containment.

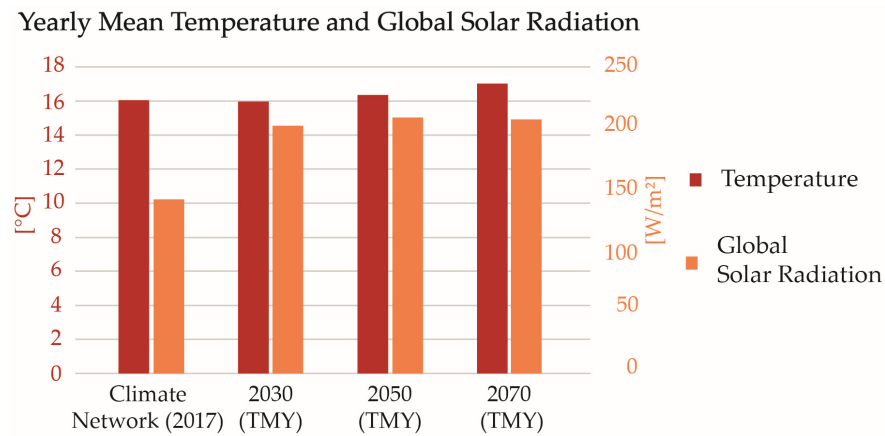


Figure 8. Yearly mean values referring to temperature and global solar radiation.

4.2. Building Energy Modelling under Future Climate Conditions

The impact of climate change was analysed, evaluating the effect that future outdoor conditions could have on the reference building in its existing and improved version. The case study’s energy performance was assessed in terms of energy consumption and thermal comfort rates. In the first case, the results refer to the annual building heating and cooling use, whereas the thermal comfort was investigated considering a weekly timestep, simulating alternatively a typical summer (August, from the 17th to 23rd) and winter (January, from the 20th to 26th) conditions. Moreover, to define comfort/discomfort rates, the operative temperature was estimated for two different building thermal zones, selected for their orientation. North- and south-exposed thermal zones were chosen to investigate winter and summer comfort, respectively. This choice was made considering the building dimensions and to prevent averaged values that did not represent the real energy behaviour.

The energy consumptions, depicted from Figures 9–11, underline a constant increase in the building cooling load and a similar decrement in the heating need, and this happens for both the original state and that with DSF configurations. Among the investigated typologies, the Multi-Storey DSF performed better than the others, allowing, at the same time, a good cooling reduction and a more intense heating decrement. Additionally, the Shaft-Box, Corridor and Box-Window configurations exhibited a general and quasi-identical energy reduction under future conditions. Moreover, significant differences were not observed for the two analysed Corridor DSFs.

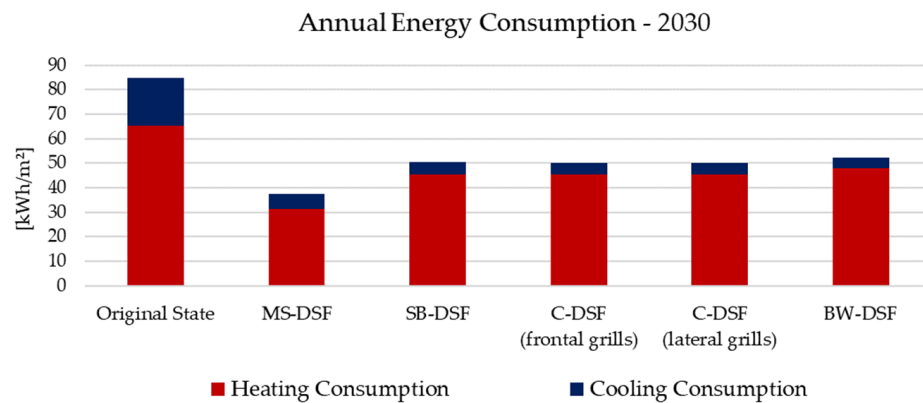


Figure 9. Building annual energy consumption estimated for the year 2030.

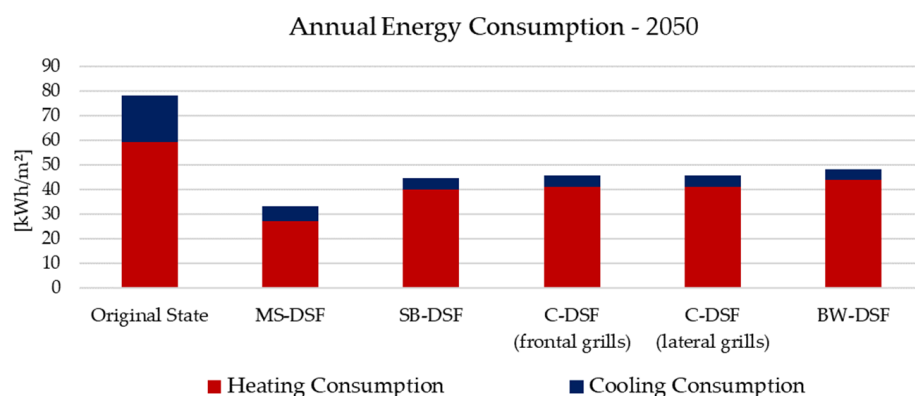


Figure 10. Building annual energy consumption estimated for the year 2050.

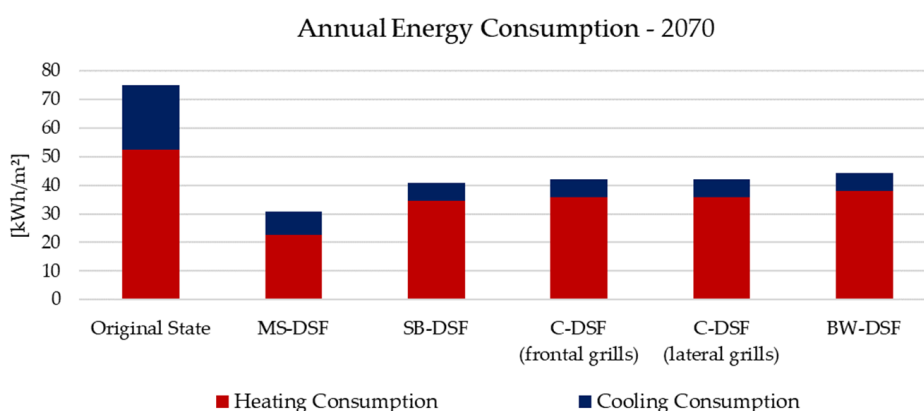


Figure 11. Building annual energy consumption estimated for the year 2070.

The evaluation of indoor thermal comfort was carried out according to the UNI EN 16798-1:2019 (CEN 2019) [59], which associates comfort/discomfort rates with four categories. In detail, Category I has a high level of expectation, and it is recommended for spaces occupied by very sensitive people. Category II is for normal levels of expectations and is suitable in the case of new buildings or renovations. Category III represents a moderate, acceptable level of expectation and can be used for existing buildings, whereas the last, Category IV, involves other conditions not covered by the previous cases. Moreover, the standard establishes for each comfort category a temperature interval, suggesting recommended indoor operative temperatures for the design of heating and cooling systems. These values are used to define each category’s upper and lower limits, as summarised in Table 3. It is essential to underline that the here-investigated parameter is a building with a heating and cooling system. Thus, the performed simulations aimed to evaluate its effectiveness in guaranteeing acceptable comfort rates inside the occupied spaces.

Table 3. Indoor operative temperature ranges for comfort categories according to the UNI EN 16798-1:2019 [59] for residential buildings.

Category	Winter Operative Temperature Range	Summer Operative Temperature Range
I	$T_{operative} \geq 21\text{ }^{\circ}\text{C}$	$T_{operative} \leq 25.5\text{ }^{\circ}\text{C}$
II	$20\text{ }^{\circ}\text{C} \leq T_{operative} < 21\text{ }^{\circ}\text{C}$	$25.5\text{ }^{\circ}\text{C} < T_{operative} \leq 26\text{ }^{\circ}\text{C}$
III	$18\text{ }^{\circ}\text{C} \leq T_{operative} < 20\text{ }^{\circ}\text{C}$	$26\text{ }^{\circ}\text{C} < T_{operative} \leq 27\text{ }^{\circ}\text{C}$
IV	$T_{operative} < 18\text{ }^{\circ}\text{C}$	$T_{operative} > 27\text{ }^{\circ}\text{C}$

The thermal comfort analysis was used to evaluate the indoor operative temperature expected for the thermal zones under study before and after the installation of the DSFs. In

detail, the operative temperature intervals for both the summer and winter periods were adopted to establish the percentage of the corresponding indoor environmental quality categories associated with each building configuration. In this specific case, only Categories II, III and IV were considered as the simulations were carried out for an existing building, and a normal level of expectation would be “Medium” (Category II), as recommended by the standard. Furthermore, the mean, minimum and maximum expected operative temperature was extracted for better comparisons. The indoor temperatures estimated for the building in its original state were assumed as baseline, and percentages of increments/decrements were calculated and are reported in the tables. The obtained categories are plotted from Figures 12–17 and the temperatures are summarised in Tables 4–9.

The comparisons underline several variations which should be taken into account for further consideration of the effectiveness of DSF systems. The estimated summer performance of Double Façades could lead to a different distribution of future comfort levels due to the high levels of predicted global solar radiation. As highlighted in the previous section, the amount of monthly mean radiation expected for the years 2030, 2050 and 2070 is much more significant than actual conditions, and this could generate the worst comfort rates for various DSF typologies. Due to a high solar load, the Double Façade, in fact, becomes a heated element which continually emits accumulated heat. This element is much more sensitive to this phenomenon than the original building envelope because it is entirely made of glazed surfaces. While on the one hand the DSF acts as a heat damper, reducing the effect of solar load on the inner operative temperature, on the other it also tends to increase the number of hours for which higher temperatures are estimated and, consequently, leads to a lower level of comfort. A mechanical system should be introduced to improve the summer indoor environment and to enhance natural ventilation in case of extra loads, converting the DSF into a hybrid technology.

In evaluating winter comfort rates (Figures 15–17), the general temperature increase predicted for the coldest months allows higher levels of expectation, and this was estimated for both the building’s original state and its state after the DSF’s installation. The discomfort rates under future conditions tend, in fact, to decrease, and this reduction assumes more significant values for DSF systems, ensuring better performances than those reachable by the reference building in its original state. Additionally, in this case, the DSF that allows the best indoor environment is the Multi-Storey variety, which is capable of guaranteeing the highest percentage with a better level of expectations. Moreover, it is interesting to note that the winter comfort level predicted for the year 2050 shows better values than 2070. This phenomenon is explained by the higher temperatures and solar radiation predicted for the investigated period (January), which positively affect the heating side, reducing its load.

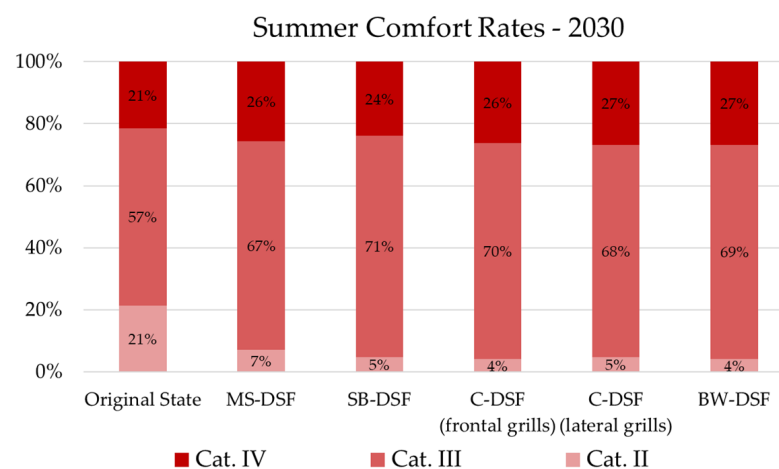


Figure 12. Comfort rates for a typical summer week according to the 2030 climatic file.

Table 4. Indoor operative mean, minimum and maximum temperature expected for a typical summer week in 2030.

Configuration	Mean Temperature	Minimum Temperature	Maximum Temperature
Original State	26.69	24.81	29.04
MS-DSF	26.72 (+0.1%)	25.44 (+2.5%)	28.00 (−3.6%)
SB-DSF	26.73 (+0.1%)	25.47(+2.7%)	27.93 (−3.8%)
C-DSF (frontal grills)	26.74 (+0.2%)	25.48(+2.7%)	28.02 (−3.5%)
C-DSF (lateral grills)	26.75 (+0.2%)	25.48 (+2.7%)	28.02 (−3.5%)
BW-DSF	26.76 (+0.3%)	25.52(+2.9%)	27.95 (−3.8%)

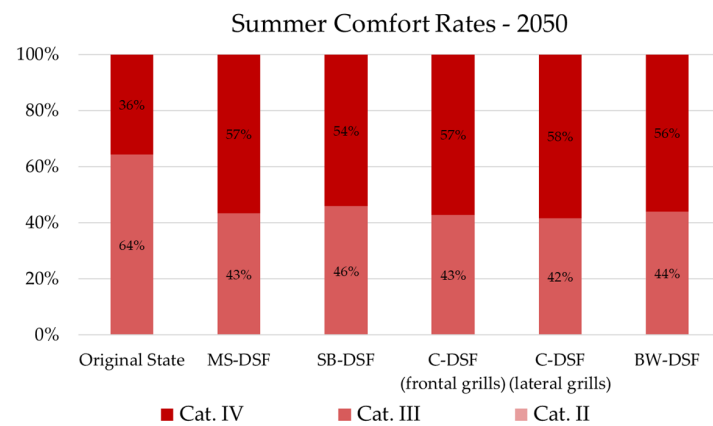


Figure 13. Comfort rates for a typical summer week according to the 2050 climatic file.

Table 5. Indoor operative mean, minimum and maximum temperature expected for a typical summer week in 2050.

Configuration	Mean Temperature	Minimum Temperature	Maximum Temperature
Original State	26.94	26.02	28.39
MS-DSF	27.07 (+0.5%)	26.54 (+2.0%)	27.78 (−2.1%)
SB-DSF	27.05 (+0.4%)	26.54 (+2.0%)	27.73 (−2.3%)
C-DSF (frontal grills)	27.08 (+0.5%)	26.58 (+2.2%)	27.79 (−2.1%)
C-DSF (lateral grills)	27.08 (+0.5%)	26.57 (+2.1%)	27.79 (−2.1%)
BW-DSF	27.06 (+0.4%)	26.57 (+2.1%)	27.74 (−2.3%)

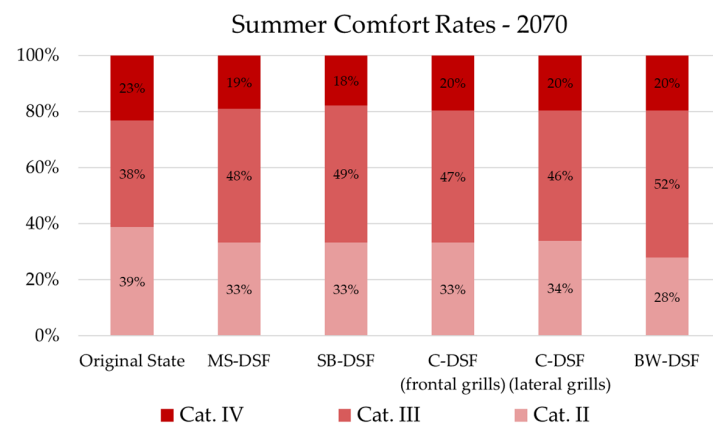


Figure 14. Comfort rates for a typical summer week according to the 2070 climatic file.

Table 6. Indoor operative mean, minimum and maximum temperature expected for a typical summer week in 2070.

Configuration	Mean Temperature	Minimum Temperature	Maximum Temperature
Original State	26.36	24.53	28.37
MS-DSF	26.41 (+0.2%)	25.05 (+2.1%)	27.82 (−1.9%)
SB-DSF	26.41 (+0.2%)	25.07 (+2.2%)	27.75 (−2.2%)
C-DSF (frontal grills)	26.43 (+0.3%)	25.06 (+2.2%)	27.82 (−1.9%)
C-DSF (lateral grills)	26.42 (+0.2%)	25.05 (+2.1%)	27.81 (−2.0%)
BW-DSF	26.44 (+0.3%)	25.11 (+2.4%)	27.76 (−2.2%)

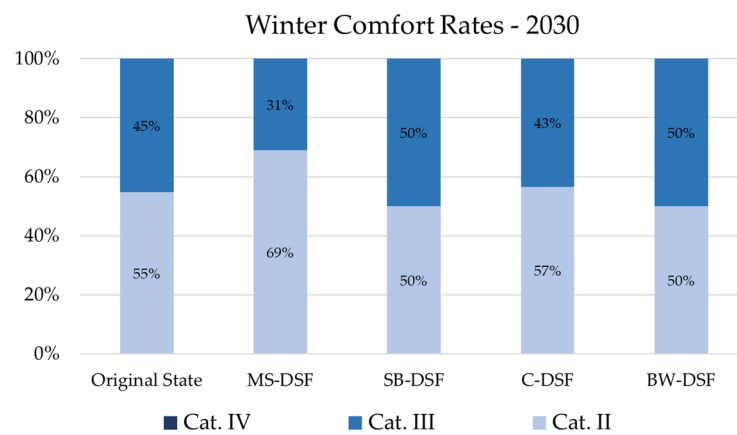


Figure 15. Comfort rates for a typical winter week according to the 2030 climatic file.

Table 7. Indoor operative mean, minimum and maximum temperature expected for a typical winter week in 2030.

Configuration	Mean Temperature	Minimum Temperature	Maximum Temperature
Original State	20.22	18.68	24.62
MS-DSF	20.50 (+1.4%)	18.92 (+1.3%)	23.83 (−3.2%)
SB-DSF	20.05 (−0.8%)	18.86 (+1.0%)	21.67 (−12.0%)
C-DSF	20.21 (+0.0%)	18.93 (+1.3%)	21.86 (−11.2%)
BW-DSF	20.05 (−0.8%)	18.84 (+0.9%)	21.59 (−12.3%)

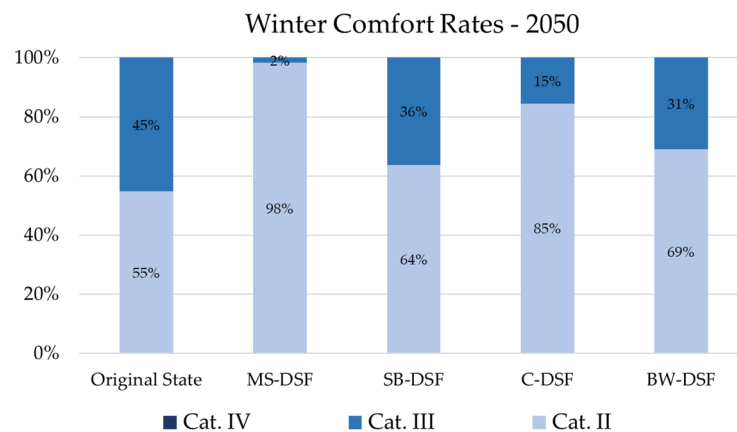
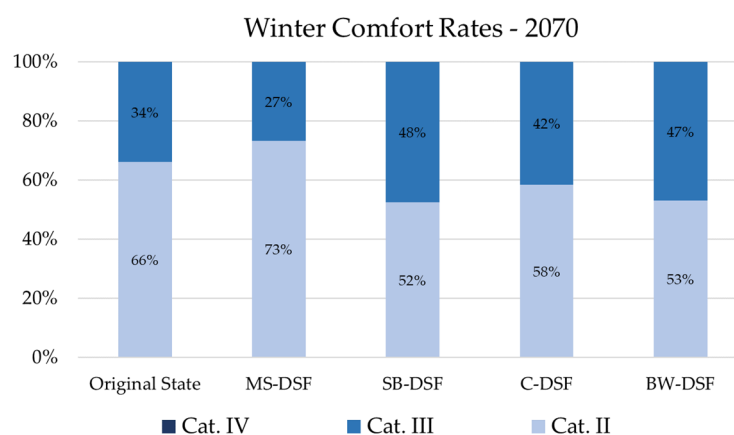


Figure 16. Comfort rates for a typical winter week according to the 2050 climatic file.

Table 8. Indoor operative mean, minimum and maximum temperature expected for a typical winter week in 2050.

Configuration	Mean Temperature	Minimum Temperature	Maximum Temperature
Original State	20.13	19.15	20.92
MS-DSF	21.72 (+7.9%)	19.88 (+3.8%)	25.61 (+22.4%)
SB-DSF	20.56 (+2.1%)	19.45 (+1.6%)	22.11 (+5.7%)
C-DSF	20.86 (+3.6%)	19.65 (+2.6%)	22.65 (+8.3%)
BW-DSF	20.59 (+2.3%)	19.49 (+1.8%)	21.98 (+5.1%)

**Figure 17.** Comfort rates for a typical winter week according to the 2070 climatic file.**Table 9.** Indoor operative mean, minimum and maximum temperature expected for a typical winter week in 2070.

Configuration	Mean Temperature	Minimum Temperature	Maximum Temperature
Original State	20.48	18.94	25.67
MS-DSF	20.74 (+1.3%)	19.14 (+1.1%)	24.27 (−5.5%)
SB-DSF	20.17 (−1.5%)	19.01 (+0.4%)	27.72 (+8.0%)
C-DSF	20.36 (−0.6%)	19.12 (+1.0%)	21.95 (−14.5%)
BW-DSF	20.18 (−1.5%)	19.01 (+0.4%)	21.64 (−15.7%)

5. Discussion

As underlined by the performed simulations, the installation of multiple DSFs in existing buildings leads to a general improvement in the energy performance with regard to both consumption and comfort. Intense heating and cooling savings are expected when comparing the building's original state and the Multi-Storey configuration. The annual heating and cooling consumption, in fact, can be cut down, respectively, to 52–57% and 65–68% for the considered year. Similar but less intense trends, especially regarding the heating requirement, were estimated for the other DSFs. The presence of horizontal or vertical partitions and the subdivision of the cavity into multiple chambers, in fact, causes a higher heating requirement and, even if they are associated with slightly better cooling needs (a reduction of 63–74% for the Shaft-Box and 68–79% for the Box-Window), the global annual energy is higher than when the Multi-Storey option is considered. The air channel increases the natural ventilation of the occupied spaces, thus reducing their temperature and, at the same time, creates a more effective barrier against heat loss throughout the building envelope during the wintertime. Finally, the two Corridor DSF versions exhibit negligible differences, underlining that the system performance is not affected by the air grills' location but is influenced by their dimensions.

The analysis of the expected thermal comfort conditions provides a few challenging aspects that should be considered in the case of DSFs. The implementation of an additional insulation layer represented by the Double-Skin Façade reduces heat transfer and ensures more stable indoor temperature fluctuations. This improvement becomes particularly noticeable during extreme meteorological conditions, such as hot summers and cold winters. As a main consequence of more uniform indoor temperatures, the discomfort conditions last longer because heat dissipation occurs slowly. For this reason, the summer comfort rate evaluation highlights higher discomfort, reaching the worst comfort categories, predicted for DSF solutions when compared to the original building state. Among the investigated options, the Multi-Storey configuration exhibits slightly better values than the others, decreasing from Category II, or 21% of the time, to 7% for 2030 and from 39% to 33% for 2070, respectively, for the existing configuration and the retrofitting one. The analysis of the indoor operative temperature confirms the above-mentioned considerations. In fact, even if the expected mean temperature is quasi-identical (a variation of about 0.1–0.5% is predicted for the selected years and configurations) among the original and energy-improved version, lower maximum temperatures were estimated in the retrofitted model (−1.9% for the Multi-Storey DSF in 2070 and up to −3.8% for the Shaft-Box DSF in 2030), confirming the effectiveness of DSFs in reducing extreme conditions.

The winter week, instead, highlights the benefits achievable by installing the multi-layer façade. In particular, the Multi-Storey configuration ensures the highest percentage of Category II, reaching 98% for 2050 but also performing well for the other years. Acceptable comfort rates are also estimated with the other configurations, especially with the Corridor DSF. Additionally, in this case, a minor temperature fluctuation is evidenced by the analyses after the installation of the Double-Skin Façade. The expected minimum operative temperature is always higher in the case of the retrofitted building than its current version, and this increment rises from 0.4% for the Shaft-Box and Box-Window configurations in 2070 up to 3.8% for the Multi-Storey configuration in 2030.

While the thermal comfort assessment results and energy savings in buildings retrofitted with Double-Skin Façades are promising, there are some limitations to consider. The study focused on a specific building type, which is largely present in existing Italian building and located in a climatic context quite representative of the Mediterranean area. Nevertheless, further research is needed to explore different climate zones, building typologies and variations in façade design to understand the broader applicability and potential challenges associated with Double-Skin Façades. Moreover, more advanced and smart ventilation systems should be introduced and analysed to tackle climate change phenomena and reduce the vulnerability of DSFs to global warming and the overheating risk of the cavity.

6. Conclusions

The present research aimed to assess the climate change vulnerability of a residential building located in Pescara, Central Italy. The energy performance of the case study was evaluated by considering its current and improved version through dynamic energy simulations. The building energy requirement, subdivided into cooling and heating needs, and the indoor thermal comfort rates were estimated under future climate conditions in order to establish the best DSF retrofit solution. Thus, typical meteorological years were generated using regional climate models, and the main weather parameters expected for 2030, 2050 and 2070 were defined.

The results underline the impact that the continuous increase in temperature and solar radiation have on building energy consumption, analysing both the heating and cooling needs. Lower winter energy loads were, in fact, estimated for the investigated years in comparison to current weather conditions. In contrast, higher cooling consumption will be necessary to ensure satisfactory comfort rates inside the occupied spaces. By inserting a DSF on the northwest and southeast elevations, energy savings can be expected, with benefits throughout the year. The installation of multi-layer façades, particularly in the Multi-Storey configuration, ensures significant reductions of up to about 52–57% and 65–68% for the

considered year, respectively, for the heating and cooling needs. Similar performances, even though they were slightly less effective overall, can be expected with the other DSFs, for which higher cooling savings were calculated for the summertime (up to 63–74% for the Shaft-Box and 68–79% for the Box-Window) and lower savings were predicated for the coldest months (with an average of 32%, 13% and 27%, for the Shaft-Box, Corridor and Box-Window configurations).

In addition to the improvements achievable on the energy side, using DSFs to restore existing buildings positively affects the comfort rates, especially during the wintertime. By reducing extreme weather peaks and, in general, temperature fluctuation, the air cavity allows more uniform conditions to be maintained than the building's current configuration. The capability of DSFs in enhancing heat dissipation directly impacts the expected indoor operative temperatures, which were calculated to be $\pm 3.8\%$ higher and lower, respectively, than the indoor minimum and maximum operative temperatures calculated for the original state. Moreover, mechanical ventilation should be introduced to prevent the summer overheating risk of the air cavity due to elevated solar radiation and temperature levels with consequently high discomfort rates expected inside the inner spaces, thus enhancing natural convection in the case of extreme thermal loads. Additionally, in this case, the configuration with the best performance was the Multi-Storey configuration.

Furthermore, Double-Skin Façades not only provide thermal benefits but also contribute to improved indoor air quality. The additional layer acts as a buffer zone and reduces outdoor air pollutants and noise infiltration, leading to a healthier and more comfortable indoor environment for occupants. Moreover, DSFs maintain adequate natural daylight penetration while minimising glare and excessive solar heat gain. This balance ensures occupants have access to natural light, reducing the reliance on artificial lighting during the day and promoting a more pleasant visual environment.

In view of the achieved results, the use of DSFs for the energy retrofit of existing buildings proves to be a suitable option, with savings in terms of energy requirements and comfort rates. Despite these achievements, there are still some knowledge gaps the remain to be filled. Among them, long-term monitoring and evaluation to understand their performance over extended periods is still required. Factors such as maintenance requirements, durability and ageing effects on thermal and optical properties need to be investigated to ensure that the expected benefits are sustained over the lifespan of the building. More research is needed to assess DSF performance variations and optimise the design for different climatic contexts and to understand the impact of Double-Skin Façades on occupant comfort during different seasons, including winter. Factors such as thermal comfort, visual comfort, acoustic performance and user preferences should be thoroughly investigated to create designs that meet both energy and comfort objectives.

Author Contributions: Conceptualization, S.M. and C.L.; methodology, S.M. and M.P.; investigation C.L.; writing—original draft preparation, C.L.; writing—review and editing, C.L., S.D.L., M.P. and S.M.; supervision, S.M. and M.P. All authors have read and agreed to the published version of the manuscript.

Funding: This research was developed within the framework of the Italian Research Project “Soluzioni integrate energetiche e antisismiche per costruzioni edili”, under the PON action “Dottorati Innovativi con caratterizzazione Industriale”, funded by the Italian Ministry for the Economic Development—CUP: D92F16000360003.

Institutional Review Board Statement: Not applicable.

Informed Consent Statement: Not applicable.

Data Availability Statement: Not applicable.

Conflicts of Interest: The authors declare no conflict of interest.

References

1. Mazzarella, L. Energy Retrofit of Historic and Existing Buildings. The legislative and Regularity Point of View. *Energy Build* **2015**, *95*, 23–31. [CrossRef]
2. European Environment Agency. *The European Environment—State and Outlook 2020. Knowledge for the Transition to a Sustainable Europe*; European Union: Brussel, Belgium, 2019; pp. 1–499.
3. Buildings Performance Institute Europe (BPIE). *Europe's Building under the Microscope. A Country-by-Country Review of the Energy Performance of Buildings*; Buildings Performance Institute: Brussel, Belgium, 2011; pp. 1–132.
4. UN Environment and International Energy Agency. *Towards a Zero-Emission, Efficient, and Resilient Buildings and Construction Sector. Global Status Report 2017*; UN Environment: Nairobi, Kenya, 2017; pp. 1–48.
5. Directive 2002/91/EC of the European Parliament and of the Council of 16 December 2002 on the Energy Performance of Buildings. *Off. J. Eur. Communities*. 2003. Available online: <http://data.europa.eu/eli/dir/2002/91/oj> (accessed on 23 January 2023).
6. Directive 2010/31/EU of the European Parliament and of the Council of 19 May 2010 on the Energy Performance of Buildings (Recast). *Off. J. Eur. Union*. 2010. Available online: <http://data.europa.eu/eli/dir/2010/31/oj> (accessed on 23 January 2023).
7. Directive 2012/27/EU of the European Parliament and of the Council of 25 October 2012 on Energy Efficiency, Amending Directives 2009/125/EC and 2010/30/EU and Repealing Directives 2004/8/EC and 2006/32/EC. *Off. J. Eur. Union*. Available online: <http://data.europa.eu/eli/dir/2012/27/oj> (accessed on 23 January 2023).
8. Buildings Performance Institute Europe (BPIE). *State of the Building Stock-Briefing*; Buildings Performance Institute: Brussel, Belgium, 2012; pp. 1–2.
9. Oh, M.; Lee, C.; Park, J.; Lee, K.; Tae, S. Evaluation of Energy and Daylight Performance of Old Office Buildings in South Korea with Curtain Walls Remodeled Using Polymer Dispersed Liquid Crystal (PDLC) Films. *Energies* **2019**, *12*, 3679. [CrossRef]
10. Moreno, Á.; Chemisana, D.; Vaillon, R.; Riverola, A.; Solans, A. Energy and Luminous Performance Investigation of an OPV/ETFE Glazing Element for Building Integration. *Energies* **2019**, *12*, 1870. [CrossRef]
11. Sethi, M.; Lamb, W.; Minx, J.; Creutzig, F. Climate change mitigation in cities: A systematic scoping of case studies. *Environ. Res. Lett.* **2020**, *15*, 1748–9326. Available online: <https://iopscience.iop.org/article/10.1088/1748-9326/ab99ff> (accessed on 27 May 2023). [CrossRef]
12. Kabisch, N.; Frantzeskaki, N.; Pauleit, S.; Naumann, S.; McKenna, D.; Artmann, M.; Haase, D.; Knapp, S.; Korn, H.; Stadler, J.; et al. Nature-based solutions to climate change mitigation and adaptation in urban areas: Perspectives on indicators, knowledge gaps, barriers, and opportunities for action. *Ecol. Soc.* **2016**, *21*, 239. [CrossRef]
13. Ricci, R.; Vitali, D.; Montelpare, S. An innovative wind-solar hybrid street light: Development and early testing of a prototype. *Int. J. Low-Carbon Technol.* **2015**, *10*, 420–429. [CrossRef]
14. Kim, D.; Cox, S.J.; Cho, H.; Yoon, J. Comparative investigation on building energy performance of double skin façade (DSF) with interior or exterior slat blinds. *J. Build. Eng.* **2018**, *20*, 411–423. [CrossRef]
15. Lucchino, E.C.; Gennaro, G.; Favoino, F.; Goia, F. Modelling and validation of a single-storey flexible double-skin façade system with a building energy simulation tool. *Build. Environ.* **2022**, *226*, 109704. [CrossRef]
16. Jankovic, A.; Goia, F. Characterization of a naturally ventilated double-skin façade through the design of experiments (DOE) methodology in a controlled environment. *Energy Build.* **2022**, *263*, 112024. [CrossRef]
17. Matour, S.; Garcia-Hansen, V.; Omrani, S.; Hassanli, S.; Drogemuller, R. Thermal performance and airflow analysis of a new type of Double Skin Façade for warm climates: An experimental study. *J. Build. Eng.* **2022**, *62*, 105323. [CrossRef]
18. Bugenings, L.A.; Schaffer, M.; Larsen, O.K.; Zhang, C. A novel solution for school renovations: Combining diffuse ceiling ventilation with double skin façade. *J. Build. Eng.* **2022**, *49*, 104026. [CrossRef]
19. Ballestini, G.; De Carli, M.; Masiero, N.; Tombola, G. Possibilities and limitations of natural ventilation in restored industrial archaeology buildings with a double-skin façade in Mediterranean climates. *Build. Environ.* **2005**, *40*, 983–995. [CrossRef]
20. Catto Lucchino, E.; Gelesz, A.; Skeie, K.; Gennaro, G.; Reith, A.; Serra, V.; Goia, F. Modelling double skin façades (DSFs) in whole-building energy simulation tools: Validation and inter-software comparison of a mechanically ventilated single-story DSF. *Build. Environ.* **2021**, *199*, 107906. [CrossRef]
21. Poirazis, H. *Double Skin Façades: A Literature Review*; Lund University, Lund Institute of Technology Department of Architecture and Built Environment: Lund, Sweden, 2006; pp. 1–252.
22. Uuttu, S. *Study of Current Structures in Double-Skin Façades*; Helsinki University of Technology: Espoo, Finland, 2001.
23. Heimrath, R.; Hengsberger, H.; Mach, T.; Streicher, W.; Waldner, R.; Flamant, G.; Loncour, X.; Guarracino, G.; Erhorn, H.; Erhorn-Kluttig, H.; et al. BESTFAÇADE. Best Practice for Double Skin Façades. WP 1 Report “State of the Art”. 2005, pp. 1–151. Available online: http://www.bestfacade.com/pdf/downloads/Bestfacade_WP1_Report.pdf (accessed on 27 May 2023).
24. Zhai, Z.; Chen, Q.; Haves, P.; Klems, J.H. On Approaches to Couple Energy Simulation and Computational Fluid Dynamics Programs. *Build Environ.* **2002**, *37*, 857–864. [CrossRef]
25. Lops, C.; Germano, N.; Ricciutelli, A.; D’Alessandro, V.; Montelpare, S. Naturally Ventilated Double Skin Façades: Comparisons Between Different CFD Models. *Math. Model. Eng. Probl.* **2021**, *8*, 837–846. [CrossRef]
26. Germano, N.; Lops, C.; Montelpare, S.; Camata, G.; Ricci, R. Determination of Wind Pattern Inside an Urban Area Through a Mesoscale-Microscale Approach. *Math. Model. Eng. Probl.* **2020**, *7*, 515–519. [CrossRef]
27. Chan, A.L.S.; Chow, T.T.; Fong, K.F.; Lin, Z. Investigation on Energy Performance of Double Skin Façade in Hong Kong. *Energy Build.* **2009**, *41*, 1135–1142. [CrossRef]

28. Gratia, E.; De Herde, A. The Most Efficient Position of Shading Devices in a Double-Skin Façade. *Energy Build.* **2007**, *39*, 364–373. [CrossRef]
29. Joe, J.W.; Choi, W.J.; Huh, J.H. Operation Strategies for an Office Building Integrated with Multi-Story Double Skin Façades in the Heating Season. In Proceedings of the Building Simulation 2011: 12th Conference of International Building Performance Simulation Association, Sydney, Australia, 14–16 November 2011.
30. Ding, W.; Hasemi, Y.; Yamada, T. Natural Ventilation Performance of a Double-Skin Façade With a Solar Chimney. *Energy Build.* **2005**, *37*, 411–418. [CrossRef]
31. Gontikaki, M. Optimization of a Solar Chimney Design to Enhance Natural Ventilation in a Multi-Storey Office Building. In Proceedings of the 10th International Conference for Enhanced Building Operations, Kuwait, 26–28 October 2010.
32. Abraham, S.B.; Ming, T.Z. Numerical Analysis on The Thermal Performance of a Building With Solar Chimney and Double Skin Façade in Tropical Country. *IOP Conf. Ser. Mater. Sci. Eng.* **2018**, *453*, 012030. [CrossRef]
33. Stec, W.J.; van Paassen, A.H.C.; Maziarz, A. Modelling the Double Skin Façade with Plants. *Energy Build.* **2005**, *37*, 419–427. [CrossRef]
34. De Gracia, A.; Navarro, L.; Castell, A.; Cabeza, L.F. Energy Performance of Ventilated Double Skin Façade with PCM Under Different Climates. *Energy Build.* **2015**, *91*, 37–42. [CrossRef]
35. Johnny, A.E.; Shanks, K. Optimization of Double-Skin Facades for High-Rise Buildings in Hot Arid Climates. *Int. J. Environ. Sustain.* **2018**, *7*, 88–100. [CrossRef]
36. Gaillard, L.; Giroux-Julien, S.; Ménézo, C.; Pabiou, H. Experimental Evaluation of a Naturally Ventilated PV Double-Skin Building Envelope in Real Operating Conditions. *Sol Energy.* **2014**, *10*, 223–241. [CrossRef]
37. Athienitis, A.K.; Buonomano, A.; Ioannidis, Z.; Kapsis, K.; Stathopoulos, T. Double Skin Façades Integrating Photovoltaics and Active Shadings: A Case Study for Different Climates. In Proceedings of the 1st International Conference on Building Integrated Renewable Energy Systems, Dublin, Ireland, 6–9 March 2017.
38. Luo, Y.; Zhang, L.; Wang, X.; Xie, L.; Liu, Z.; Wu, J.; Zhang, Y.; He, X. A comparative study on thermal performance evaluation of a new double skin façade system integrated with photovoltaic blinds. *Appl. Energy* **2017**, *199*, 281–293. [CrossRef]
39. Jayathissa, P.; Luzzatto, M.; Schmidli, J.; Hofer, J.; Nagy, Z.; Schlueter, A. Optimising Building Net Energy Demand With Dynamic BIPV Shading. *Appl. Energy* **2017**, *202*, 726–735. [CrossRef]
40. Moon, K.S. Structural Design of Double Skin Facades as Damping Devices for Tall Buildings. *Procedia. Eng.* **2011**, *14*, 1351–1358. [CrossRef]
41. Zhang, R. SMART BUILDINGS: An Integrative Double Skin Façade Damper System For Structural Safety and Energy Efficiency. Ph.D. Dissertation, University of New Hampshire, Durham, UK, 2017.
42. Takeuchi, T.; Yasuda, K.; Iwata, M. Studies on Integrated Building Facade Engineering with High-Performance Structural Elements. *IABSE Symp. Rep.* **2006**, *92*, 33–40. [CrossRef]
43. Scuderi, G. Adaptative Exoskeleton for the Integrated Retrofit of Social Housing Buildings. Ph.D. Dissertation, University of Trento, Trento, Italy, February 2016.
44. Passoni, C.; Belleri, A.; Marini, A.; Riva, P. Sustainable Restoration of Post-WWII European Reinforced Concrete Buildings. In Proceedings of the 16th World Conference on Earthquake, Santiago, Chile, 9–13 January 2017.
45. Labò, S. Holistic Sustainable Renovation of Post-World War II Reinforced Concrete Building Under A Life Cycle Perspective by Means Diagrid Exoskeletons. Ph.D. Dissertation, University of Bergamo, Bergamo, Italy, March 2019.
46. Khabir, S.; Vakilnezhad, R. Energy and thermal analysis of DSF in the retrofit design of office buildings in hot climates. *Archit. Eng. Des. Manag.* **2022**, *1–23*. [CrossRef]
47. Ascione, F.; Bianco, N.; Iovane, T.; Mastellone, M.; Mauro, G.M. The evolution of building energy retrofit via double-skin and responsive façades: A review. *Solar Energy* **2021**, *224*, 703–717. [CrossRef]
48. Sarihi, S.; Mehdizadeh Saradj, F.; Faizi, M. A Critical Review of Façade Retrofit Measures for Minimizing Heating and Cooling Demand in Existing Buildings. *Sustain. Cities Soc.* **2021**, *64*, 102525. [CrossRef]
49. Montelpare, S.; D’Alessandro, V.; Lops, C.; Costanzo, E.; Ricci, R. A Mesoscale-Microscale approach for the energy analysis of buildings. *J. Phys. Conf. Ser.* **2019**, *1224*, 012022. [CrossRef]
50. Peel, M.C.; Finlayson, B.L.; McMahon, T.A. Updated World Map of the Köppen-Geiger Climate Classification. *Hydrol. Earth Syst. Sci.* **2007**, *11*, 1633–1644. [CrossRef]
51. Fondazione Osservatorio Meteorologico Milano Duomo ETS. Available online: <https://www.fondazioneomd.it/climate-network> (accessed on 20 January 2019).
52. Giorgi, F.; Jones, C.; Asrar, G.R. Addressing climate information needs at the regional level: The CORDEX framework. *World Meteorol. Organ. Bull.* **2019**, *58*, 175.
53. Bubnovà, R. Integration of the Fully Elastic Equations Cast in the Hydrostatic Pressure Terrain-Following Coordinate in the Framework of the ARPAGE/Aladin NWP SYstem. *Am. Meteorol. Soc.* **1995**, *123*, 515–535. [CrossRef]
54. Farda, A.; Déu, M.; Somot, S.; Horányi, A.; Spiridonov, V.; Tóth, H. Model ALADIN as Regional Climate Model for Central and Eastern Europe. *Stud. Geophys. Geod.* **2010**, *54*, 313–332. [CrossRef]
55. Horanyi, A.; Ihasz, I.; Radnoti, G. ARPEGE/ALADIN: A numerical Weather Prediction Model for Central-Europe with the Participation of the Hungarian Meteorological Service. *Időjárás* **1996**, *100*, 277–301.

56. Huth, R.; Mládek, R.; Metelka, L.; Sedlák, P.; Huthová, Z.; Kliegrová, S.; Kyselý, J.; Pokorna, L.; Helenka, T.; Janoušek, M. On the Integrability of Limited-Area Numerical Weather Prediction Model ALADIN over Extended Time Periods. *Stud. Geophys. Geod.* **2003**, *47*, 863–873. [[CrossRef](#)]
57. *EN ISO 15927-4:2005*; Hygrothermal Performance of Buildings—Calculation and Presentation of Climatic Data—Part 4: Hourly Data for Assessing the Annual Energy Use for Heating and Cooling. ISO: Geneva, Switzerland, 2005.
58. Cebecauer, T.; Suri, M. Typical Meteorological Year Data: SolarGIS Approach. *Energy Procedia* **2015**, *69*, 1958–1969. [[CrossRef](#)]
59. *UNI EN 16798-1:2019*; Energy Performance of Buildings—Ventilation for Buildings-Part 1: Indoor Environmental Input Parameters for Design and Assessment of Energy Performance of Buildings Addressing Indoor Air Quality, Thermal Environment, Lighting and Acoustics—Module M1-6. Ente Nazionale Italiano di Unificazione (UNI): Milano, Italy, 2019.

Disclaimer/Publisher’s Note: The statements, opinions and data contained in all publications are solely those of the individual author(s) and contributor(s) and not of MDPI and/or the editor(s). MDPI and/or the editor(s) disclaim responsibility for any injury to people or property resulting from any ideas, methods, instructions or products referred to in the content.